Spin−Orbit Configuration Interaction Calculation of the Potential Energy Curves of Iodine Oxide

S. Roszak,[†,‡] M. Krauss,[§] A. B. Alekseyev,*[,‡] H.-P. Liebermann,[‡] and R. J. Buenker[‡]

Institute of Physical and Theoretical Chemistry, Wroclaw University of Technology, Wyb. Wyspianskiego 27, 50-370 Wroclaw, Poland; Fachbereich 9—Theoretische Chemie, Bergische Universität-Gesamthochschule Wuppertal, Gaussstr. 20, D-42097 Wuppertal, Germany; and Center for Advanced Research in Biotechnology, NIST, 9600 Gudelsky Drive, Rockville, Maryland 20850

Received: November 10, 1999; In Final Form: January 27, 2000

An ab initio configuration interaction (CI) study including spin−orbit coupling is carried out for the ground and excited states of the IO radical by employing relativistic effective core potentials. The computed spectroscopic constants are in good agreement with available experimental data, with some tendency to underestimate the strength of bonding. The first excited state, $a^4\Sigma^-$, which has not yet been observed experimentally, is predicted to be bound by 30.1 kJ/mol and to have a significantly larger equilibrium distance than the ground state. It is split by spin−orbit interaction into $^1/_2$ and $^3/_2$ components, with the $^1/_2$ component being the lower one with a calculated spin−orbit splitting of 210 cm^{-1}. The most interesting state in the low-energy IO spectrum, $A_1{}^2\Pi_{3/2}$, is shown to be predissociated due to interaction with a number of repulsive electronic states. Predissociation of the A_1, $v' = 0$, 1 vibrational levels is attributed to a fairly weak spin−orbit coupling with the $^2\Delta_{3/2}$ state, while rotationally dependent predissociation of the $v' = 2$ level is explained by the coupling with the $^1/_2$(III) state having mainly $^2\Sigma^-$ character. Strong predissociation of the $v' \geq 4$ levels is attributed to interaction with the higher-lying $\Omega = {}^3/_2$ states, with predominantly $^4\Sigma^+$ and $^4\Delta$ origin.

1. Introduction

The halogen oxides play an important role in atmospheric chemistry. Neutral IO is formed in the reaction of iodine with ozone, resulting in the destruction of ozone in the troposphere.[1] It is known that the oceans are a significant source of iodine to the atmosphere,[1−4] primarily in the form of CH_3I, which is rapidly photolyzed in the troposphere to release iodine atoms. Salomon et al.[5] speculated that catalytic reactions of the IO radical could be at least partly responsible for the depletion of lower stratospheric O_3 and sudden episodic ozone disappearance in the Arctic troposphere during the springtime. As a result, the kinetics and mechanisms of reactions involving IO have been studied in a number of laboratories.[6−14] The physical properties of the isolated IO molecule have also been studied intensively.[15−18] A critical review of experimental thermochemical data on IO is also available.[19]

Despite the large interest in IO, theoretical studies are scarce and restricted to its ground electronic state.[20−22] The qualitative picture of excited electronic states in IO can be inferred from the states in ClO.[23] An important conclusion is that the excited $A^2\Pi$ state in ClO dissociates to an excited atomic asymptote, $O(^1D)$, and thus must be bound, though strongly predissociated by the repulsive valence states going to the lowest $Cl(^2P^o) + O(^3P)$ atomic limit. From the numerous spectroscopic studies it is well-known that this is also true for the heavier halogen monoxides and the dominant transition in all these systems was found to be the $A^2\Pi_{3/2}-X^2\Pi_{3/2}$.[24−27] The emission spectra of IO were observed early on from methyl iodide flames[28,29] and were analyzed in more detail in later high-resolution and laser-induced fluorescence (LIF) studies.[6−8,24−26] The absorption $A^2\Pi_{3/2} \leftarrow X^2\Pi_{3/2}$ spectra have also been studied often.[9,14,27,30−34] The $X^2\Pi_{1/2}$ state is not found in absorption because of the large spin−orbit splitting in the ground electronic state.[16] A recent study of the A state[27] found that predissociation in the $v' = 0,3$ levels is independent of rotation, while $v' = 2$ is rotationally predissociated and the remaining observed vibrational levels, $v' = 1,4,5$, are so diffuse that the mode of predissociation could not be determined. It was suggested that the rotational predissociation was caused by coupling to the $^2\Sigma^-$ state, while the other vibrational states were predominantly dissociated by repulsive $\Omega = {}^3/_2$ states.

In the present work we report calculated potential energy curves for the ground and excited states of IO. The excited IO states are calculated for the first time and provide data for analysis of the low-energy IO spectra and for identification of states which perturb the $A^2\Pi_{3/2}$ state.

2. Computational Method

In the present theoretical treatment the core electrons of the iodine atom are described by a relativistic effective core potential (RECP) given by LaJohn et al.[35] and only the 4d, 5s, and 5p shells are treated explicitly via basis functions. The 1s shell of the oxygen atom is also described by a core potential.[36] The original (4s4p) basis set[36] for the oxygen atom was taken in an uncontracted form and augmented by two d polarization functions (with exponents 2.314 and 0.645). The original (3s3p4d) basis set[35] for the iodine atom was contracted to [3s3p2d] (three largest d exponents contracted) and supplemented with one f polarization function (0.44) and s, p Rydberg primitive functions (both exponents equal to 0.021).

* Author for correspondence. E-mail: alexeev@uni-wuppertal.de.
† Wroclaw University of Technology.
‡ Bergische Universität-Gesamthochschule Wuppertal.
§ NIST.

10.1021/jp994002l CCC: $19.00
Published on Web 03/11/2000

TABLE 1: Technical Details of the MRD-CI Calculations of IO at $T = 0.3$ μH[a]

C_{2v} sym	N_{ref}/N_{root}	SAFTOT/SAFSEL	$C_{\infty v}$ notation	$\sum c_p^2$
$^2B_{1,2}$	53/4	2 422 179/148 310	$^2\Pi(4)$	0.902
$^2A_1$	44/3	1 588 047/132 444	$^2\Sigma^+$, $^2\Delta(2)$	0.896
$^2A_2$	43/4	2 011 674/125 114	$^2\Sigma^-(2)$, $^2\Delta(2)$	0.898
$^4B_{1,2}$	34/3	2 077 799/153 791	$^4\Pi(3)$	0.886
$^4A_1$	26/3	1 760 522/140 061	$^4\Sigma^+$, $^4\Delta(2)$	0.903
$^4A_2$	50/4	2 226 888/164 658	$^4\Sigma^-(2)$, $^4\Delta(2)$	0.893

[a] The number of selected SAFs and the $\sum c_p^2$ values over reference configurations (for the lowest root of each symmetry) are given for $r = 3.60$ a_0. SAFTOT designates the total number of generated, SAFSEL the number of selected SAFs, N_{ref} and N_{root} refer to the number of reference configurations and roots treated, respectively.

The first step in the present study is a self-consistent-field (SCF) calculation of the $...\pi^4\sigma^2\pi^{*4}$ $^1\Sigma^+$ state of IO^-. Such a choice of the calculated state at the SCF level yields molecular orbitals (MOs) of the proper symmetry for the correlation procedures. Both the SCF and the CI calculations are carried out with the spin-independent part of the RECP and include all relativistic effects other than spin−orbit coupling, which is only introduced at the last stage. Results are obtained at a series of intermolecular distances ranging from 3.0 to 10.0 a_0.

The standard multireference single- and double-excitation CI method (MRD-CI)[37,38] is employed throughout for the Λ−S calculations. A series of key reference configurations is defined for a number of low-lying electronic states of a given Λ−S symmetry from which all singly and doubly excited configurations are generated. The Table CI algorithm[39] is used for efficient handling of the complicated open-shell relationships which arise in such an approach. A perturbative selection procedure is then employed to reduce the sizes of the secular equations solved in each case. Energy results at the unselected level of treatment are obtained by an extrapolation procedure,[37] while the effects of higher excitations (estimated full CI energies) are taken into account via a multireference generalization of the Davidson correction.[40−42] All calculations are carried out in the C_{2v} subgroup, although the SCF-MOs themselves transform as irreducible representations of the full $C_{\infty v}$ linear group. Details regarding the numbers of reference configurations and roots treated for each of 21 Λ−S states (doublets and quartets) are given in Table 1. Sizes of the corresponding generated and selected CI spaces are also presented, as well as the $C_{\infty v}$ notation and the $\sum c_p^2$ values of the reference configuration coefficients in the final CI eigenfunctions for the lowest roots of each irreducible representation.

The final step in the present method is to employ the Λ−S eigenfunctions as basis for the spin−orbit CI calculations. The estimated full CI energies described above are placed on the diagonal of the Hamiltonian matrices, whereas off-diagonal matrix elements are obtained by employing pairs of selected CI wave functions with $M_s = S$ and applying spin-projection techniques and the Wigner-Eckart theorem. More details of the spin−orbit CI approach may be found elsewhere.[43,44]

The CI calculations were performed for three roots in $^2A_1$ symmetry and four roots in each of $^2A_2$, $^2B_1$, and $^2B_2$ symmetries as well as for three A_1, four A_2, and three B_1 and B_2 quartet states. Such a choice includes all electronic states originating from the ground states of oxygen (^3P) and iodine ($^2P^o$). Two additional roots for $^2B_{1,2}$ and one additional root for each other symmetry type were also included. The present $^3P-^1D$ splitting for oxygen (17 306 cm^{-1}), calculated for an I−O separation of 10.0 bohr, reproduces the experimental value of 15 754 cm^{-1} reasonably well,[45] whereby one expects an overestimation of this quantity based on consideration of correlation effects. The calculated spin−orbit splitting for the iodine $^2P^o$ term obtained for the same I−O separation is 7372 cm^{-1}, as compared with the experimental value of 7603 cm^{-1}.[45]

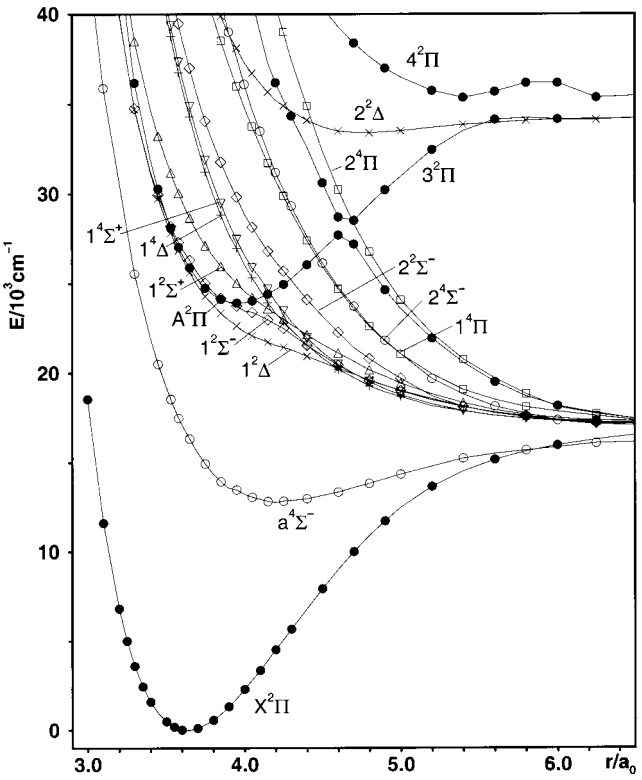

Figure 1. Potential energy curves of the low-lying Λ−S states of the IO radical calculated without including spin−orbit coupling.

3. Potential Energy Curves

The Λ−S potential energy curves calculated without including spin−orbit coupling are shown in Figure 1. The $X^2\Pi$ ground state has a $...\sigma^2\pi^4\pi^{*3}$ leading configuration. The σ and π orbitals have bonding character, while the π^* orbital is antibonding. The first excited state, $a^4\Sigma^-(\sigma^2\pi^4\pi^{*2}\sigma^*)$, arises from the $\pi^* \rightarrow \sigma^*$ excitation and is characterized by much weaker bonding and significantly larger equilibrium distance, indicating that the σ^* orbital is much more antibonding than the π^*. This is also illustrated by the fact that three other states having the same $\sigma^2\pi^4\pi^{*2}\sigma^*$ leading configuration, $^2\Delta$, $^2\Sigma^-$, and $^2\Sigma^+$, are all repulsive (see Figure 1). It is worth noting that admixtures of the $\sigma^2\pi^3\pi^{*3}\sigma^*$ configuration to the above three states are not negligible at the equilibrium distance of the ground state (about 5−6%) and become larger at $r \geq 4.0$ a_0 (around 20%), which is important for the analysis of the $A_1{}^2\Pi_{3/2}$ rotational predissociation. The only other bound electronic state in the low-energy IO spectrum is $A^2\Pi$. It is characterized by a $\sigma^2\pi^3\pi^{*4}$ leading configuration near its equilibrium distance and converges diabatically to the first excited dissociation limit, $I(^2P^o) + O(^1D)$. As can be seen from Figure 1, it exhibits an avoided crossing with the third $^2\Pi(\sigma\pi^4\pi^{*3}\sigma^*)$ state near 4.7 a_0, which leads to a maximum on the $A^2\Pi$ potential curve and its adiabatic dissociation to the ground state atomic products, $I(^2P^o) + O(^3P)$. Altogether there are 12 Λ−S states converging to this dissociation limit, and those which have not been mentioned yet, $1^4\Delta$, $1^4\Sigma^+$, $2^2\Sigma^-$, and $2^4\Sigma^-$, are characterized by a $\sigma^2\pi^3\pi^{*3}\sigma^*$ main configuration, while the two lowest $^4\Pi$ states come from $\sigma\pi^4\pi^{*3}\sigma^*$ and $\sigma^2\pi^3\pi^{*2}\sigma^{*2}$, respectively. The three lowest-lying Λ−S states correlating with the $I(^2P^o) + O(^1D)$ asymptote are

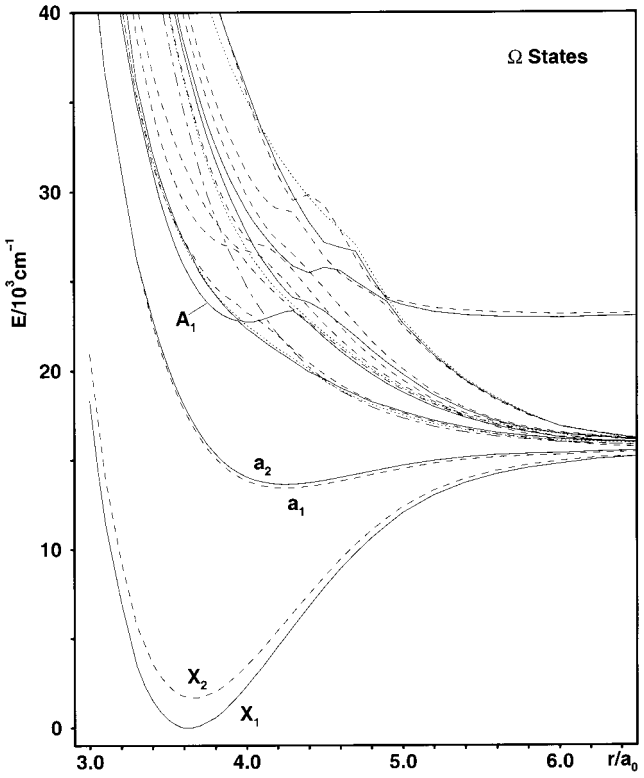

Figure 2. Potential energy curves for the lowest electronic states of the IO radical calculated including spin−orbit coupling (solid lines for $\Omega = {}^3/_2$ states, dashed lines for $\Omega = {}^1/_2$, dotted lines for $\Omega = {}^5/_2$, and a dot−dashed line for $\Omega = {}^7/_2$).

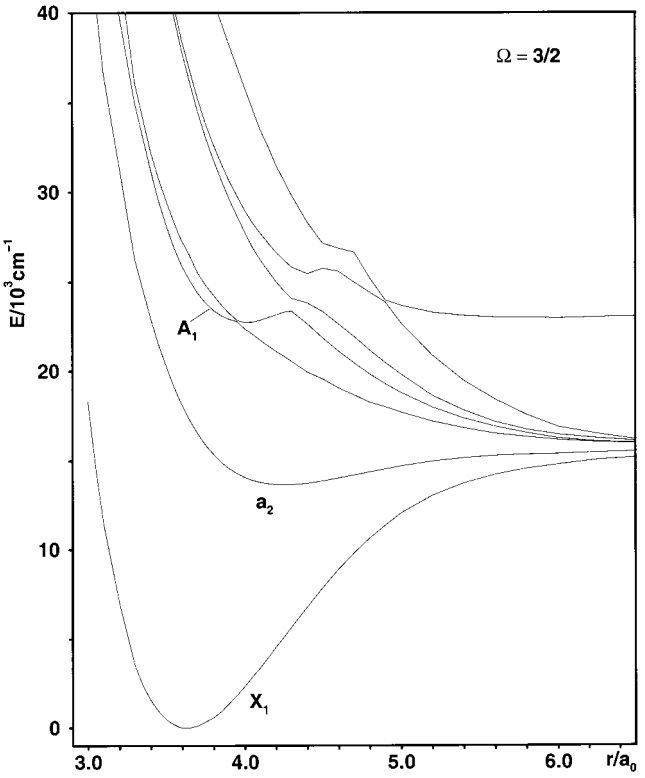

Figure 3. Computed potential energy curves for $\Omega = {}^3/_2$ states.

also shown in Figure 1. They are the $3^2\Pi$ state, already mentioned, as well as $2^2\Delta(\sigma^2\pi^3\pi^{*3}\sigma^*)$ and $4^2\Pi(\sigma^2\pi^4\pi^*\sigma^{*2})$.

Spin−orbit interaction, which is quite strong in the IO radical due to the presence of the heavy I atom, yields numerous Ω states, shown together in Figure 2 and separately in Figure 3 for the $\Omega = {}^3/_2$ states, which are of special interest for this system. All 18 Ω states which dissociate to the three lowest $I(^2P^o_{3/2}) + O(^3P_J)$ atomic limits are presented in Figure 2, with 10, 6, and 2 states going to the $O(^3P_J)$ asymptotes with $J = 2$, 1, and 0, respectively. In addition, the two lowest $^3/_2$ and $^1/_2$ states converging to the $I(^2P^o_{1/2}) + O(^3P_2)$ limit are shown. Computed spectroscopic parameters for the low-lying bound Ω states are given in Table 2 along with experimental and previous calculated data for the ground state.

The inverted doublet $X_1{}^2\Pi_{3/2}$ ground state of IO was confirmed by EPR[46] and ESR[47] measurements. The dissociation energy for this state has been determined by many different techniques. The values may be grouped into two types: (1) those derived from the treatment of the observed energy levels and (2) those extracted from kinetic studies. The various investigations are not in good agreement with each other, with experimental values ranging from 176 to 249 kJ/mol.[19] The heats of formation of IO derived theoretically[20,21] also differ substantially. The present calculated results of 206 kJ/mol (at the Λ−S) and 191 kJ/mol (including the spin−orbit interaction) lie well within the experimental error bars. The multireference CI calculations are known to give some underestimation of the ground state dissociation energy, normally by 5−20 kJ/mol, so that the above value of 191 kJ/mol may be considered as the lower limit for this quantity.The spin−orbit coupling for the ground state leads to a T_e splitting of 1683 cm^{-1}. At the experimental bond distance, the splitting is calculated to be 1867 cm^{-1}, in somewhat better agreement with the experimental value of 2091(40) cm^{-1}.[16] The upper $X_2{}^2\Pi_{1/2}$ component is calculated to have a slightly longer (by ≈0.02 Å) equilibrium distance and somewhat smaller vibrational frequency (by 24 cm^{-1}) than the $X_1{}^2\Pi_{3/2}$ ground state, which is in very good agreement with the experimental findings and indicates that the relative accuracy of the present calculation is noticeably better than the absolute one. The bond distances calculated in the present study are uniformly too large by ≃0.05 Å, which we attribute to the fact that the iodine d electrons have been frozen at the CI stage of the calculations and to a lesser extent to deficiencies in the RECPs employed and basis set errors.

TABLE 2: Calculated and Experimental Spectroscopic Properties of IO (Transition Energies T_e, Bond Lengths r_e, and Vibrational Frequencies ω_e)

	T_e /cm^{-1}		r_e /Å		ω_e /cm^{-1}	
state	calc	exp	calc	exp	calc	exp
$X_1{}^2\Pi_{3/2}$	0	0	1.922	1.8677[a]	650	681.6[a]
			1.894[b]		664[b]	
$X_2{}^2\Pi_{1/2}$	1683	2091[c]	1.939	1.887[c]	626	658[c]
$a_1{}^4\Sigma^-_{1/2}$	13 430		2.249		288	
$a_2{}^4\Sigma^-_{3/2}$	13 640		2.250		287	
$A_1{}^2\Pi_{3/2}$	22 724[d]	21 558[e]	2.115	2.072[e]	514	514.5[e]

[a] Reference 26. [b] Calculated without including spin−orbit coupling in ref 22. [c] Reference 16. [d] Spectroscopic constants are calculated for the diabatic $A^2\Pi_{3/2}$ state in the internuclear distance interval of 3.7−4.3 a_0. [e] Reference 24.

The first excited state, $a^4\Sigma^-$, has a much flatter potential than the ground state and is characterized by a spin−orbit splitting of only 210 cm^{-1}, with the $\Omega = {}^1/_2$ component being the lower one. The much smaller splitting than that for the ground state can be easily understood from the predominantly Σ character of the a state. The dissociation energy of the $a_1{}^4\Sigma^-_{1/2}$ can be estimated as the energy difference at the minimum of the potential curve and at $r = 10.0\ a_0$, which gives 30.1 kJ/mol for this quantity.

The $A_1{}^2\Pi_{3/2}$ state is the most interesting species in the low-energy IO spectrum since, as described in the Introduction, it

TABLE 3: Composition of the Lowest $\Omega = {}^3/_2$ States of IO (c^2, %) at Various Bond Distances r[a]

$\Omega = 3/2$	r/a_0	$1^2\Pi$	$2^2\Pi$	$1^2\Delta$	$1^4\Sigma^+$	$1^4\Sigma^-$	$1^4\Pi$	$1^4\Delta$
$X_1{}^2\Pi_{3/2}$	3.1	99.5						
	3.6	98.5						
	4.0	96.7						
	5.0	80.1				13.7		
$a_2{}^4\Sigma^-_{3/2}$	3.1					99.1		
	3.6					97.5		
	4.0				2.1	95.1		
	5.0	7.8			11.9	72.2		4.6
3/2(III)	3.1			98.0				
	3.4		86.5	12.5				
	3.6		94.5	3.8				
	3.95		67.9	29.4	1.5			
	4.2			78.2				18.5
	5.0			51.7	18.1			21.2
3/2(IV)	3.1		97.9					
	3.4		11.5	85.3				
	3.6		1.5	94.8				
	3.95		27.0	59.4	1.6			10.3
	5.0			9.6	25.2	4.5[b]	34.2	22.3
3/2(V)	3.3							94.7
	3.6				54.7		2.9	40.4
	4.25		7.2	5.9	36.7		11.0	33.6
	5.0		5.9	4.4	8.7	52.0[b]	17.0	8.5

[a] Entries are only made for contributions with $c^2 \geq 1.0\%$. [b] Contributions from the higher-lying roots of this symmetry are included.

TABLE 4: Composition of the Lowest $\Omega = {}^1/_2$ States of IO (c^2, %) at Various Bond Distances r[a]

$\Omega = 1/2$	r/a_0	$1^2\Pi$	$2^2\Pi$	$1^2\Sigma^+$	$1^2\Sigma^-$	$1^4\Sigma^+$	$1^4\Sigma^-$	$1^4\Pi$	$1^4\Delta$
$X_2{}^2\Pi_{1/2}$	3.1	99.6							
	3.6	98.8							
	4.0	97.4							
	5.0	84.0					6.4		6.3
$a_1{}^4\Sigma^-_{1/2}$	3.1			2.9			96.7		
	3.6			2.8			96.4		
	4.0			3.1			95.3		
	5.0	3.7		7.2			81.9		
1/2(III)	3.1			6.6	92.4				
	3.6			12.7	82.3				
	4.0			15.0	72.7	8.2			2.1
	5.0			13.2	37.1[b]	29.5			19.9
1/2(IV)	3.3		96.7						
	3.6		96.5						
	3.9		90.7						5.6
	4.0			68.6	10.7[b]	9.3	2.3	3.4	
	5.0			34.1	4.5[b]	13.7		34.2	6.6
1/2(V)	3.1		87.4	10.4					
	3.6			82.1	13.3	2.1			
	4.0		63.8		4.2[b]	5.6		19.7	
	5.0			20.0	24.6[b]	7.6		43.2	

[a] Entries are only made for contributions with $c^2 \geq 2.0\%$. [b] Contributions from the higher-lying roots of this symmetry are included.

has been observed many times in emission and absorption, and the A_1-X_1 spectrum is used for identification of the IO radical in the atmosphere. It is well-known from the experimental studies that the A_1 state is strongly predissociated, probably due to interactions with a variety of electronic states, as indicated by the marked dependence of the predissociation rate on the A_1 vibrational quantum number. As one can see from Figures 2 and 3, the A_1 state indeed exhibits numerous avoided and unavoided crossings near its minimum. The avoided crossing with the lowest energy occurs at around 3.95 a_0 and is caused by spin−orbit coupling with the $1^2\Delta$ state. This interaction is relatively weak ($\langle 2^2\Pi|H_{so}|1^2\Delta\rangle = 148$ cm^{-1} at $r = 3.95$ a_0) and thus results in a sharply avoided crossing leading to adiabatic dissociation of the third $\Omega = {}^3/_2$ state to $I(^2P^o_{3/2}) + O(^3P_2)$. In fact, the energy difference between the third and fourth $^3/_2$ states is only 68 cm^{-1} at the crossing point due to the fairly complicated composition of these states, as can be seen from Table 3. Therefore, it is more convenient to consider the spin−orbit coupling between these states as a perturbation of the A_1 diabatic potential curve. Spectroscopic constants calculated for this diabatic A_1 state in the I−O distance interval from 3.7 to 4.25 a_0 are given in Table 2. An overestimation of the A_1 state's T_e value is an acceptable error for this type of calculation, but it makes quantitative analysis of the predissociation processes quite difficult. The calculated r_e value for the A_1 state is approximately 0.04 Å larger than the experimental result, with such an error also being typical for the present treatment. The calculated ω_e value agrees very well with the measured result of 514.5 cm^{-1}. Such close agreement is undoubtedly fortuitous, but it indicates once again that the overall shape the A_1 curve is probably calculated much more accurately than are the corresponding T_e and r_e values. One can also note that transitions to the $1^2\Delta_{3/2}$ state (the fourth $\Omega = {}^3/_2$ potential curve in Figure 3) are probably responsible for the underlying continuum observed recently in absorption.[33] The second avoided crossing of the $A_1{}^2\Pi_{3/2}$ state with the $^3/_2$(V) state occurs at ≈4.25 a_0. The spin−orbit interaction is much stronger in this case, because the $^3/_2$(V) state has the largest Λ−S contributions from the $1^4\Sigma^+$ and $1^4\Delta$ states (Table 3), both coming from the $\sigma^2\pi^3\pi^{*3}\sigma^*$ configuration, which differs from the $A^2\Pi$ leading configuration $\sigma^2\pi^3\pi^{*4}$ by only a single excitation. This leads to strong repulsion between the corresponding $^3/_2$ states and must result in heavy predissociation of the A_1 state. The depth of the A_1 diabatic potential up to the maximum at $r \approx 4.25$ a_0 is estimated to be about 700 cm^{-1}, which is enough to accommodate only two vibrational levels. If we assume, however, that this state should be approximately 1200 cm^{-1} deeper, which corresponds to the overestimation of its T_e value, then it would support four vibrational levels, with strong predissociation taking place for $v' \geq 4$. This supposition agrees well with the experimental findings. One can also speculate that the strong predissociation of the $v' = 1$ level, for which, similarly as for $v' \geq 4$, no rotational structure could be observed,[27] is caused by the crossing of the A_1 potential curve by the $1^2\Delta$ repulsive curve at approximately this energy. Then the best candidate for rotational predissociation of the $v' = 2$ level is the $^1/_2$(III) state (see Figure 2), which has fairly complicated Λ−S character, with the $1^2\Sigma^-$ state giving the main contribution (see Table 4 and the discussion at the beginning of this section). Rotational predissociation of the $A_1{}^2\Pi_{3/2}$ state by the first $\Omega = {}^5/_2$ state (mainly $1^2\Delta$, but with a 20% contribution from the $\sigma^2\pi^3\pi^{*3}\sigma^*$ configuration) must be of comparable probability to that by the $1^2\Sigma^-$ state. Because of the fact that the spin−orbit (homogeneous) interaction with $1^2\Delta_{3/2}$ (with nearly the same energy as $1^2\Delta_{5/2}$) is notably stronger, the latter effect is probably difficult to observe, however. Note that predissociation of the $A_1{}^2\Pi_{3/2}$ state cannot be caused by a crossing with the $\Omega = {}^7/_2$ state, which lies next in energy, because of the $\Delta\Omega = 0, \pm 1$ selection rule. Predissociation by the higher-lying states with $\Omega \neq {}^3/_2$ (see Figure 2) must be negligible in comparison with the strong homogeneous predissociation by the $^3/_2$(V) state discussed above.

Finally, one can also give a qualitative explanation for the fact that the upper $\Omega = {}^1/_2$ component of the $A^2\Pi$ state has not yet been observed. As can be seen from Figure 2, this state, ${}^1/_2$(IV), lies approximately 3800 cm^{-1} higher than A_1 ${}^3/_2$ state at $r = 3.95$ a_0 and does not form any potential well owing to strong interactions with the other ${}^1/_2$ states, which are numerous at this excitation energy. In other words, according to the present calculated data, the very strong predissociation of this state must make its spectroscopic observation very difficult.

4. Conclusion

Potential energy curves for halogen oxides are important for modeling processes in atmospheric chemistry. We report in the present study the first ab initio calculation of potential energy curves for the excited states of the IO radical. The ground electronic state is an inverted $X^2\Pi$. This state is well separated from all excited electronic states and preserves its Π character along the dissociation pathway. The calculated $X_1{}^2\Pi_{3/2}$ ground-state dissociation energy of 206 and 191 kJ/mol (spin−orbit coupling included) lies within the range indicated by available experimental studies.

The lowest excited state, $a^4\Sigma^-$, is calculated to be bound, though much more weakly so ($D_e = 0.31$ eV $= 30.1$ kJ/mol) than the ground state and has a minimum which is strongly shifted to larger distances. It still awaits experimental observation, probably as a consequence of the quite small electronic transition moment ($\langle X_1{}^2\Pi_{3/2}|\mu_z|a_2{}^4\Sigma^-_{3/2}\rangle = 0.050$ ea_0 at 3.6 a_0) connecting it with the ground state, as well as of unfavorable Franck−Condon factors.

The $\Omega = {}^3/_2$ component of the second available $^2\Pi$ electronic state is calculated to lie 22 724 cm^{-1} above the ground state, in an area densely populated with other electronic states. The spin−orbit interaction causes mixing of this state with other closely lying states, leading to a very complicated appearance of the Ω potential curves (Figures 2, 3). The relatively weak coupling with the $1^2\Delta$ electronic state is probably responsible for predissociation of the lowest A_1 vibrational levels, $v' = 0,1$, while much stronger coupling with the fifth and sixth ${}^3/_2$ states, which have predominantly $1^4\Sigma^+$ and $1^4\Delta$ character, must lead to fast predissociation of the $v' \geq 4$ levels. The most probable candidate for inducing the experimentally observed rotational predissociation of the A_1, $v' = 2$ level is the ${}^1/_2$(III) state, which has a fairly complicated $\Lambda-S$ composition in the relevant distance range, with the strongest contribution coming from the $1^2\Sigma^-$ state.

A quantitative description of the $A_1{}^2\Pi_{3/2}$ predissociation, as well as of various radiation processes in the IO radical, requires more extensive ab initio calculations, which are currently in progress.

Acknowledgment. This research was supported in part by European Science Foundation through REHE grant N 9-97 and by the Deutsche Forschungsgemeinschaft within the Schwerpunktprogramm *Theorie relativistischer Effecte in der Chemie und Physik schwerer Elemente*.

References and Notes

(1) Chameides, W. L.; Davis, D. D. *J. Geophys. Res*. **1980**, *85*, 7383.
(2) Reifenhauser, W.; Heuman, K. G. *Atmos. Environ. A* **1992**, *26*, 2905.
(3) Klick, S.; Abrahamson, K. J. *Geophys. Res*. **1992**, *97*, 12683.
(4) Alicke, B.; Hebestreit, K.; Stutz, J.; Platt, U. *Nature* **1999**, *397*, 572.
(5) Salomon, S.; Garcia, R. R.; Ravishankara, A. R. J. *Geophys. Res.* **1994**, *99*, 20491.
(6) Inoue, G.; Suzuki, M.; Washida, N. *J. Chem. Phys*. **1983**, *79*, 4730.
(7) Turnipseed, A. A.; Gilles, M. K.; Burkholder, J. B.; Ravishankara, A. R. *Chem. Phys. Lett*. **1995**, *242*, 427.
(8) Gilles, M. K.; Turnipseed, A. A.; Burkholder, J. B.; Ravishankara, A. R. *Chem. Phys. Lett*. **1997**, *272*, 75.
(9) Harwood: M. H.; Burkholder, J. B.; Hunter, M.; Fox, R. W.; Ravishankra, A. R. *J. Phys. Chem. A* **1997**, *101*, 853.
(10) Turnipseed, A. A.; Gilles., M. K.; Burkholder, J. B.; Ravishankara, A. R. *J. Phys. Chem. A* **1997**, *101*, 5517.
(11) Gilles, M. K.; Turnipseed, A. A.; Burkholder, J. B.; Ravishankara, A. R.; Salomon, S. *J. Phys. Chem. A* **1997**, *101*, 5526.
(12) Bedjanian, Y.; Le Bras, G.; Poulet, G. *J. Phys. Chem*. **1996**, *100*, 15130.
(13) Bedjanian, Y.; Le Bras, G.; Poulet, G. *Chem. Phys. Lett.* **1997**, *266*, 233.
(14) Atkinson, D. B.; Hudgens, J. W.; Orr-Ewing, A. J. *J. Phys. Chem. A* **1999**, *103*, 6173.
(15) Saito, S. *J. Mol. Spectrosc*. **1973**, *48*, 530.
(16) Gilles, M. K.; Polak, M. L.; Lineberger, W. C. *J. Chem. Phys.* **1991**, *95*, 4723.
(17) Gilles, M. K.; Polak, M. L.; Lineberger, W. C. *J. Chem. Phys.* **1992**, *96*, 8012.
(18) Zhang, Z,; Monks, P. S.; Stief, L. J.; Liebman, J. F.; Huie, R. E.; Kuo, S. C.; Klemm, R. B. *J. Chem. Phys*. **1996**, *100*, 63.
(19) Chase, M. W. *J. Phys. Ref. Data* **1996**, *25*, 1297.
(20) McGrath, M. P.; Rowland, F. S. *J. Phys. Chem.* **1996**, *100*, 4815.
(21) Hassanzadeh, P.; Irikura, K. K. *J. Phys. Chem. A* **1997**, *101*, 1580.
(22) Hassanzadeh, P.; Irikura, K. K.; Johnson, R. D., III *J. Phys. Chem. A* **1997**, *101*, 6897.
(23) Arnold, J. O.; Whiting, E. E.; Langhoff, S. R. *J. Chem. Phys*. **1977**, *66*, 4459.
(24) Durie, R. A.; Legay, F.; Ramsay, D. A. *Can. J. Phys.* **1960**, *38*, 444.
(25) Barnett, M.; Cohen, E. A.; Ramsay, D. A. *Can. J. Phys.* **1981**, *59*, 1908.
(26) Bekooy, J. P.; Meerts, W. L.; Dymanus, A. *J. Mol. Spectrosc*. **1983**, *102*, 320.
(27) Newman, S. M.; Howie, W. H.; Lane, I. C.; Upson, M. R.; Orr-Ewing, A. J. *J. Chem. Soc., Faraday Trans.* **1998**, *94*, 2681.
(28) Vaidya, W. M. *Proc. Indian Acad. Sci. A* **1937**, *6*, 122.
(29) Coleman, E. H.; Gaydon, A. G.; Vaidya, W. M. *Nature* **1948**, *162*, 108.
(30) Durie, R. A.; Ramsay, D. A. *Can. J. Phys.* **1958**, *36*, 35.
(31) Cox, R. A.; Coker, G. B. *J. Phys. Chem*. **1983**, *87*, 4478.
(32) Stickel, R. E.; Hynes, A. J.; Bradshaw, J. D.; Chameides, W. L.; Davis, D. D. *J. Phys. Chem*. **1988**, *92*, 1862.
(33) Laszlo, B.; Kurylo, M. J.; Huie, R. F. *J. Phys. Chem.* **1995**, *99*, 11701.
(34) Loewenschuss, A.; Miller, J. C.; Andrews, L. J. *Mol. Spectrosc.* **1980**, *81*, 351.
(35) LaJohn, L. A.; Christiansen, P. A.; Ross, R. B.; Atashroo, T.; Ermler, W. C. *J. Chem. Phys.* **1987**, *87*, 2812.
(36) Pacios, L. F.; Christiansen, P. A. *J. Chem. Phys.* **1985**, *82*, 2664.
(37) Buenker, R. J.; Peyerimhoff, S. D. *Theor. Chim. Acta* **1974**, *35*, 33.
(38) Buenker, R. J.; Peyerimhoff, S. D.; Butscher, W. *Mol. Phys.* **1978**, *35*, 771.
(39) Buenker, R. J.; Phillips, R. A. *J. Mol. Struct. (THEOCHEM)* **1985**, *123*, 291.
(40) Davidson, E. R. In *The World of Quantum Chemistry*; Daudel, R., Pullman, B., Eds.; Reidel: Dordrecht, 1974; p 17.
(41) Hirsch, G.; Bruna, P. J.; Peyerimhoff, S. D.; Buenker, R. J. *Chem. Phys. Lett*. **1977**, *52*, 442.
(42) Knowles, D. B.; Alvarez-Collado, J. R.; Hirsch, G.; Buenker. R. J. *J. Chem. Phys.* **1990**, *92*, 585.
(43) Alekseyev, A. B.; Liebermann, H.-P.; Buenker, R. J.; Hirsch, G.; Li, Y. *J. Chem. Phys.* **1994**, *100*, 8956.
(44) Alekseyev, A. B.; Liebermann, H.-P.; Buenker, R. J.; Hirsch, G. *J. Chem. Phys.* **1994**, *100*, 2989.
(45) Moore, C. E. *Tables of Atomic Energy Levels*; National Bureau of Standards: Washington, DC, 1971.
(46) Carrington, A.; Dyer, P. N.; Levy, D. H. *J. Chem. Phys.* **1970**, *52*, 309.
(47) Brown, J. M.; Byfleet, C. R.; Howard, B. J.; Russel, D. K. *Mol. Phys.* **1972**, *23*, 457.